PUBLISHED PROJECT REPORT PPR894

Road surface properties and high speed friction - The effect of permeability

P D Sanders

Report details

Report prepared for:	Highways England, Pavements	
Project/customer reference:	519(4/45/12)HALC	
Copyright:	© TRL Limited	
Report date:	2017	
Report status/version:	Final	
Quality approval:		
Peter Sanders (Project Manager)	**Approved**	Martin Greene (Technical Reviewer)	**Approved**

Disclaimer

This report has been produced by TRL Limited (TRL) under a contract with Highways England. Any views expressed in this report are not necessarily those of Highways England.

The information contained herein is the property of TRL Limited and does not necessarily reflect the views or policies of the customer for whom this report was prepared. Whilst every effort has been made to ensure that the matter presented in this report is relevant, accurate and up-to-date, TRL Limited cannot accept any liability for any error or omission, or reliance on part or all of the content in another context.

When purchased in hard copy, this publication is printed on paper that is FSC (Forest Stewardship Council) and TCF (Totally Chlorine Free) registered.

Table of Contents

Executive summary

In the UK the risk posed to motorists from low levels of pavement skid resistance is managed through a policy that requires direct measurement of sideway-force skid resistance, the inference of high speed friction through the measurement of road surface texture depth, and the provision of appropriately selected aggregates. The ability to infer high speed friction was a result of work published in TRL report 367 (Roe, et al., 1998) which provided a relationship between texture depth and high speed friction.

It has been shown that the relationship developed as part of TRL report 367 is capable of characterising the performance of the majority of surfacing materials, but not all. Some porous asphalt surfacings and small aggregate thin surface course systems do not follow the same texture/friction relationship as the majority of surfacing types, leading to the under-prediction of the performance of these materials.

This study follows on from an initial study into the performance of the materials mentioned above reported in TRL report PPR727 (Sanders, et al., 2014). Based on the work reported in PPR727 the following hypothesis was formed; a pavement may remove water from the tyre road interface either via the surface texture depth or through the internal permeability of the surfacing; both mechanisms aid the pavement in providing high speed locked-wheel friction. It is the aim of the work reported here to test this hypotheses through the following research tasks:

- Completion of a laboratory study initiated as part of the work reported in PPR727. The laboratory testing was aimed at characterising the permeability of a variety of thin surface course systems.

- Quantify the relationship between texture depth, permeability and high speed friction. This was achieved by using the results of the laboratory measurements and from full scale measurements of texture depth and high speed friction.

- Validate the results from the laboratory and full scale testing. This was carried out by imaging the internal structure of the specimens assessed using a CT scanner. The images were used to quantify the amount of voids through which water could escape the tyre surface interface.

From the work carried out the following conclusions can be made:

- A key characteristic influencing high speed locked-wheel friction in wet conditions is the ability of the pavement to remove water from the tyre / road interface.

- The major pathway for water removal from the tyre / road interface is through the surface texture, but the inter-connected void network can provide additional drainage routes.

- There is an indication that pavements with a large percentage of voids inevitably possess a large number of inter-connected voids.

- There is the possibility of amending current standards which require measurements of high speed friction, to allow an inference of high speed friction based on the measurement of texture and permeability.

1 Background and introduction

This chapter summarises salient historical research and current UK standards to add context to the work. The aims of the research are presented at the end of the chapter.

1.1 The relationship between texture depth and high speed friction

Fundamental research into road surface properties and pavement skid resistance was carried out in 1966 and is reported in RRL report No. 20 (Sabey, 1966). This research demonstrated a tentative correlation between the texture depth of road surfaces, (measured using the volumetric patch test), and skid resistance, (measured using the small braking force trailer). Figure 1-1 is a replication of the results reported in RRL20, a positive trend is observed between texture depth and braking force, particularly at higher speeds.
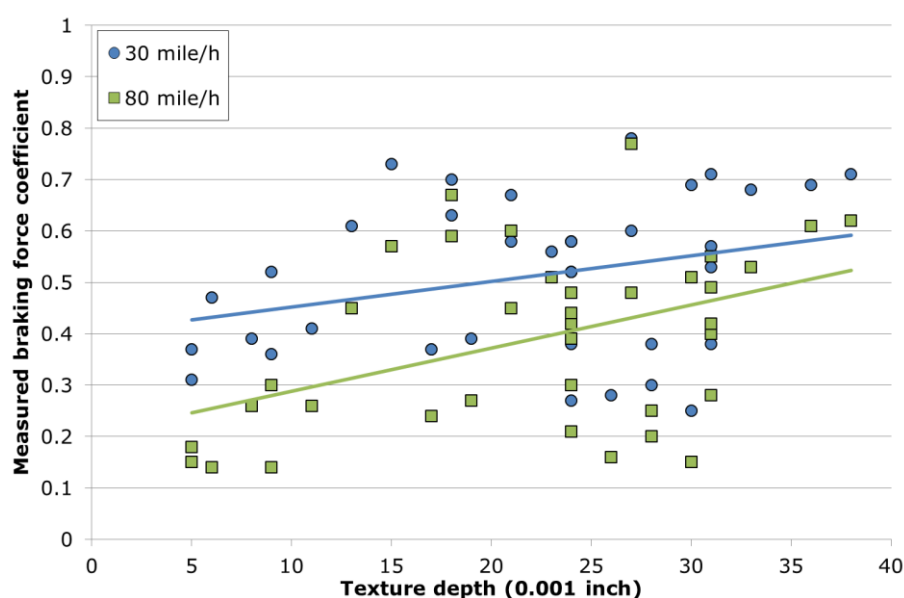
Figure 1-1 Comparison between texture depth and braking force coefficient, replicated from (Sabey, 1966)

Based on these results, Sabey concluded that:

"Very large decreases in coefficient between 30 and 80 mile/h can be expected when the texture depth is less than 0.010 in, however high the coefficient is at 30 mile/h. In order to restrict the decrease to 25 percent it appears that, on average, texture depths greater than 0.025 in are desirable." (Sabey, 1966).

Subsequent research was conducted in the USA in 1978 by Leu and Henry (1978) who conducted a statistical analysis of high speed friction, texture depth and microtexture measurements made on 20 locations in West Virginia in 1976. The researchers found correlations between texture depth, microtexture, speed and friction. The result of the work was the formulation of a friction prediction model commonly known as the Penn State model.

$$SN = SN_0 exp[-(PSNG/100) \times V]$$

Where:

- SN_0 = zero speed intercept (related to microtexture)

- PSNG = Percentage speed number gradient (related to texture depth)

Equation 1-1 The Penn State model (Leu & Henry, 1978)

Further research was conducted in 1998 by Roe, Parry and Viner and is reported in TRL report 367 (Roe, et al., 1998). This work consisted of making measurements of texture depth (using the Sensor Measured Texture Depth (SMTD) method (section 2.4)), side-force coefficient (using the side-force method (section 2.3)) and high speed friction (using the Pavement Friction Tester (PFT) (section 2.2)). The measurements made were used to develop a model capable of predicting locked-wheel friction at 100 km/h (L-Fn100) based on measurements of side-force coefficient and texture depth, Equation 1-2.

$$L - Fn100 = aSR + b(1 - e^{SMTD}) + c$$

Where:

- a, b and c are the model coefficients[1]

- SR represents the side-force coefficient measured using SCRIM

- SMTD is the texture depth of the surface measured using the SMTD method.

Equation 1-2 Prediction for L-Fn100 (Roe, et al., 1998)

It is interesting to note that the exponential function is raised to a power proportional to texture depth in both Equation 1-1 and Equation 1-2.

1.2   The identification of outlying materials

An additional observation from the work reported in TRL367 is shown in Figure 1-2 which shows the individual texture and high speed friction measurements made, categorised by material type. In general the measurements are concentrated in a narrow band which increases linearly between 0 and 0.70 mm SMTD and is flat thereafter. However the group of points at approximately 0.75 mm SMTD and 0.50 Fn at 100 km/h are outlying from the main band of measurements. The report authors noted that:

"It is possible that there are some different mechanisms involved in that way in which these materials interact with the tyre to generate friction. However it is more likely that, however it is that SMTD measures on porous surfacings, this measure of texture depth does not adequately represent the texture. For example, such surfacings have clearly have a greater

---

[1] The model coefficients were not stated in TRL367 but these have been provided by one of the authors, a = 0.00337, b = 0.411 and c = -0.151.

drainage potential than SMTD (or sand patch) measurements of texture depth can quantify."
(Roe, et al., 1998)
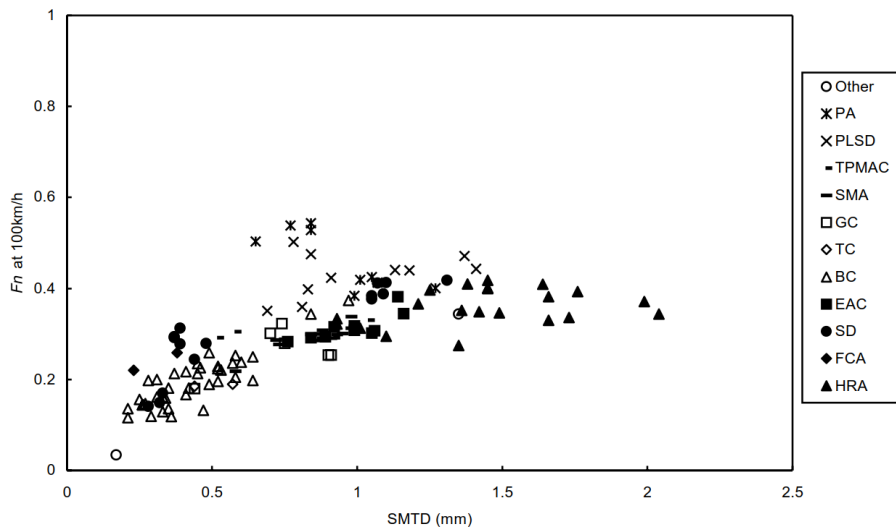
Figure 1-2 Comparison of texture and high speed friction (Roe, et al., 1998)

Research reported in TRL report PPR564 (Roe & Dunford, 2012) has identified another material type, a 6 mm Thin Surface Course System (TSCS), which displays similar properties to the porous asphalt identified in TRL367. This work made measurements of high speed friction (using the PFT) and texture depth (using the SMTD method) on TSCSs with different course aggregate sizes.   A summary of the measurements made as part of PPR564 is replicated from the original data in Figure 1-3. Included in this figure are the data from TRL367, represented by the grey series markers.
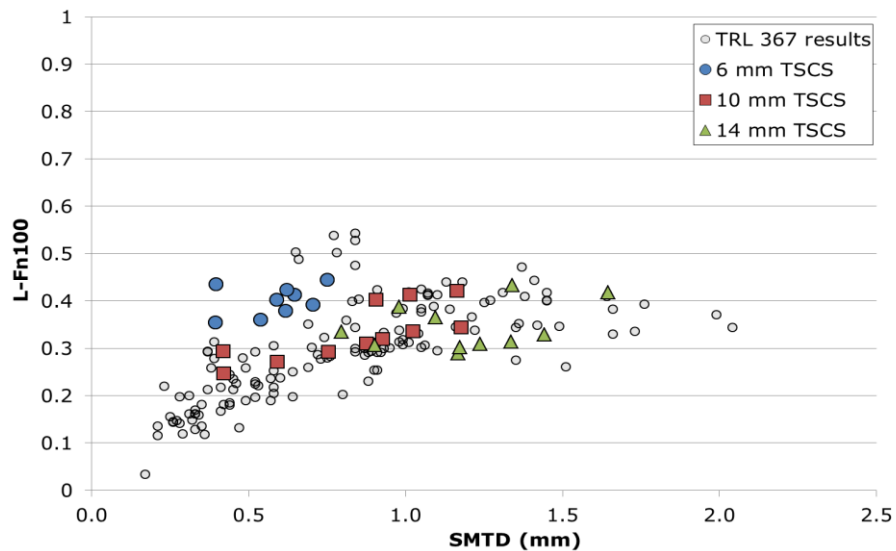
Figure 1-3 Texture and high speed friction on different TSCS materials, replicated from (Roe & Dunford, 2012) and (Roe, et al., 1998)

Figure 1-3 shows that, of the materials assessed, the materials constructed from the 10 mm and 14 mm nominal aggregate sizes are performing within the range of the results from the study reported in TRL367. The materials using a nominal 6 mm aggregate size are showing a similar performance to the outlying measurements to the TRL 367 results in that they are providing higher levels of friction than would be expected from their texture depth values.

1.3 Current UK texture depth requirements

1.3.1 Initial texture depth requirements

In the light of the findings of PPR564 the standards governing the application of TSCS materials, the MCHW 900 series (2008) were updated by way of an Interim Advice Note (IAN) in 2012. IAN 154/12 (2012) allows the use of lower levels of texture depth on 6 mm thin surface course systems than were required before the publication of PPR564. Table 1-1 and Table 1-2 present the pertinent texture information from IAN 154/12; the bold boxes in both tables represent the information pertaining to 6 mm TSCSs.

Table 1-1 Requirements for initial texture depth for trunk roads including motorways (MCHW 900 series) and (IAN 154/12)

Road	Average MTD per 1,000 m section, mm	
	MCHW 900 Series	IAN154
High speed roads Posted speed limit ≥ 50 miles/hr (80 km/h)	≥1.3	≥1.0 and ≤1.5
Lower speed roads Posted speed limit ≥ 40 miles/hr (65 km/h)	≥1.0	≥1.0 and ≤1.5
Roundabouts on high speed roads Posted speed limit ≥ 50 miles/hr (80 km/h)	≥1.2	≥1.2 and ≤1.7
Roundabouts on lower speed roads Posted speed limit ≥ 40 miles/hr (65 km/h)	≥1.0	≥1.0 and ≤1.5

Table 1-2 Requirements for retained texture depth for trunk roads including motorways (MCHW 900 series) and (IAN 154/12)

Surfacing type	Average MTD per 1,000 m section, mm[A]	
	MCHW 900 Series	IAN154
Hot applied thin surface course systems with an upper (D) aggregate size of 14 mm	1.0	0.9
Hot applied thin surface course systems with an upper (D) aggregate size of 10 mm	1.0	0.8
Hot applied thin surface course systems with an upper (D) aggregate size of 6 mm	1.0	0.7[B]

A - or the complete carriageway lane where this is less than 1,000 m.

B - Verification of high speed friction performance required.

Table 1-1 and Table 1-2 demonstrate the relaxing of requirements applied to 6 mm TSCSs; this relaxation was granted on the basis of the research presented at the start of this chapter. However, full confidence in the performance of the 6 mm TSCSs could not be established as part of the previous work and in order to fail safe, the requirement was added for these materials to demonstrate their high speed friction performance after being laid.

1.3.2   In service requirements

The in-service performance of road pavements in the UK is governed by the documents comprising the Design Manual for Roads and Bridges (DMRB). HD 29/08 (2008) of the DMRB provides details of the texture depth requirements. In summary a TRAffic speed Condition Survey (TRACS) survey makes SMTD measurements which are compared to threshold values (shown in Table 1-3) which define the deterioration category of the road (described in Table 1-4).

Table 1-3 Texture depth category thresholds (HD 29/08)

Category	1	Threshold value	2	Threshold value	3	Threshold value	4
Texture depth (mm)							
Anti-skid surfacing (HFS)		0.6		N/A		N/A	
All other surfaces		1.1		0.8		0.4	

Table 1-4 TRACS category definitions (HD 29/08)

Category	Description
1	Sound – no visible deterioration.
2	Some deterioration – lower level of concern. The deterioration is not serious and more detailed (project level) investigations are not needed unless extending over long lengths, or several parameters are at this category at isolated positions.
3	Moderate deterioration – warning level of concern. The deterioration is becoming serious and needs to be investigated. Priorities for more detailed (scheme level) investigations depend on the extent and values of the condition parameters.
4	Severe deterioration – intervention level of concern. This condition should not occur very frequently on the motorway and all purpose trunk road network as earlier maintenance must have prevented this state from being reached. At this level of deterioration more detailed (scheme level) investigations should be carried out on the deteriorated lengths at the earliest opportunity and action taken if, and as, appropriate.

As can be deduced from Table 1-3 and Table 1-4, in order for a road to require no further investigation, it must provide a texture depth (SMTD) of 0.8 mm or greater. However as demonstrated by Figure 1-3 only the best performing 6 mm TSCS materials are likely to provide this level of texture depth. Furthermore, there is no mechanism within this

standard to account for the improved high speed friction performance demonstrated by these materials.

1.4   Initial investigation

An initial investigation into the behaviour of these 6mm TSCS materials was commissioned in 2013 with a view to developing a new texture depth characterisation that would account for the discrepancy in friction performance. This work was reported in TRL report PPR727 (Sanders, et al., 2014).

The investigation utilised historical high speed friction measurements collected using the PFT. These measurements were made on a variety of sites containing thin surface course materials. In the work reported in PPR727 these high speed friction measurements acted as reference measurements, against which various pavement parameters would be assessed.

The work showed that it was not possible to identify a texture measurement technique capable of fully characterising the performance of 6 mm TSCS materials. As part of that study a small number of laboratory assessments were carried out into the relationship between the porosity of the specimens and their high speed friction. The results of this aspect of the study were positive and indicated that with further porosity assessments the nature of the performance of 6 mm TSCS materials might be understood. It is the aim of the work reported in this document to complete the further work recommended by the initial investigation.

1.5   Research aims

The hypothesis for this work is that a pavement may remove water from the tyre road interface either via the surface texture depth or through the internal permeability of the material; both mechanisms aid the pavement in providing high speed locked-wheel friction.

Testing of this hypothesis was undertaken through the following research tasks:

- Completion of the laboratory assessments initiated as part of the work reported in PPR727.

- Quantifying the relationship between texture depth, permeability and high speed friction.

- Validating the results from the laboratory and full scale testing by imaging the internal structure of the specimens used in the laboratory testing.

2 Completion of the texture, permeability and high speed friction assessment

The data used for this work were originally collected as part of the works reported in PPR324 (Roe, et al., 2008), PPR564 (Roe & Dunford, 2012) and PPR727 (Sanders, et al., 2014). The following sections present the measurement methods used for each of the material properties and summarise the materials assessed.

2.1 Materials assessed

The materials assessed for this work were originally the subject of research published in PPR324 (Roe, et al., 2008) which provides detailed information for each of the materials. The materials were all laid between 2005 and 2007 at various locations in the UK, detailed site maps are provided in Appendix A and Table 2-1 provides a summary. All of the materials are TSCSs utilising different nominal coarse aggregate sizes.

Table 2-1 Summary of materials assessed

Site Number	Section	Coarse aggregate size (mm)	Lane(s)	Road	Direction	Location
1	1	10	1 & 2	A5	WB	Gibbet Hill, Lutterworth, Leicestershire
	2	6				
	3	14				
2	1	14	1 & 2	A5	WB	Tamworth, Staffordshire
	2	10				
3	1	14	1	A14	WB	Creeting St Mary, Suffolk
	2	10				
	3	6				
4	1	14	1 & 2	A43	NB	Brackley, Northamptonshire
	2	10				
	3	20				
	4	6				
5[2]	1	6	1	A14	EB	Thrapston, Northamptonshire
	2	10				
	3	14				
	4	6				
	5	10				
	6	14				
6	1	6	1 & 2	A14	EB	Stanford-on-Avon, Northamptonshire
	2	10				
	3	14				

[2] This site contains two material types with the same coarse aggregate size.

To allow for laboratory assessment, two specimens (150mm diameter cores) were removed from each section. The specimens were removed after the collection of high speed friction, side-force skid resistance, and texture information. In total, 60 specimens were used in this work for the assessment of pavement porosity. For clarity, the pavement from which individual cores were extracted will be referred to as the parent surface, and the cores, the specimens.

2.2   High speed friction

High speed friction measurements were made on each parent surface with the 1295 Pavement Friction Tester (PFT) (Figure 2-1), a locked-wheel friction testing device owned by Highways England and operated on their behalf by TRL. The PFT consists of a tow vehicle (1995 Chevrolet Silverado), and test trailer which employs the locked-wheel technique allowing it to measure the friction generated between the test tyre and road surface throughout the complete braking cycle. This allows the determination of the peak[3] and locked-wheel[4] friction for the speed at which the test was carried out.

Figure 2-1 The Pavement Friction Tester (PFT)

Measurements were made under the advice of ASTM E-274 (ASTM, 2011) using the tyre specified in ASTM E-524 (ASTM, 2008). Wet conditions were achieved by pumping water (from a tank in the tow vehicle), at a controlled rate. This results in a nominal water film of 1.0 mm between the tyres contact point and pavement surface.

---

[3] The maximum amount of friction generated between the tyre and surface.

[4] The amount of friction generated between the tyre and surface when the test wheel is in the fully locked condition.

Peak and locked-wheel friction were measured at various speeds ranging from 20 km/h to 120 km/h. A regression analysis was then used to identify the locked-wheel friction values at 100 km/h reported as L-Fn100. The use of the L-Fn100 allowed the measurements to be compared with the results of TRL367.

2.3   Side-force coefficient

The Sideway-force Coefficient Routine Investigation Machine (SCRIM) is the standard device for monitoring the side-force coefficient condition of the UK trunk road network, and is also used by many local authorities. Figure 2-2 shows the Highways England SCRIM which was used for this work, this device has now been decommissioned.

Figure 2-2 The Highways England SCRIM device

SCRIM uses a smooth test tyre angled at 20 degrees to the direction of travel, mounted on an instrumented axle to record a SCRIM Reading (SR) for every 10 m length of road. The SR is the average ratio between the measured sideway-force and the vertical load, which is dynamically measured, multiplied by 100. Measurements of sideway-force coefficient were made using SCRIM on each of the parent surfaces. The measurements were made at a test speed of 50 km/h and are reported in this document as SR(50).

2.4   Texture depth

Measurements of texture depth were made on each parent surface using the Sensor Measured Texture Depth (SMTD) method. The SMTD method uses a triangulation laser fitted to a vehicle (the HE SCRIM device) to make measurements of the displacement between the sensor receiver and road surface as the vehicle travels down the road at traffic speed. The distance measurements are combined with speed information to provide a two dimensional profile of the road surface. SMTD values were provided as 10 m average values and the mean of these values was used as the indicative texture depth of each section.

2.5   Permeability

The assessment of pavement permeability was carried out on the specimens removed from each of the sites in Table 2-1.   The methodology described in BS EN 12697-19:2012 (British Standards, 2012) was used. This methodology can be summarised as applying a constant hydrostatic head of water to the surface of each specimen and allowing the water to exit the specimen through the side only. The permeability of the specimen was calculated by collecting the ejected water over a known period of time and recording the mass of the collected water.

To achieve this, a steel tube was bonded to a specimen surface, and the outside edge of the top of the specimen was sealed using silicone sealant. This isolated the surface texture and allowed water to escape the surface only through the specimen. The bottom of the specimen was also sealed to reduce any effect of drainage relating to variations in the amount of binder course still attached to the surface course.

Water with a constant hydrostatic head of 2.94 N/m^2 was fed into the steel tube and allowed to flow through the specimen to saturate the voids in the specimen. Once saturated, the water flowing out of the specimen was collected over a known period of time and the flow rate calculated using the mass of the collected water. The resulting volumetric flow rate is therefore indicative of the amount of horizontal permeability within the specimen which in turn is a characterisation of the amount of inter-connected voids in the specimen. The equipment used is shown in Figure 2-3.
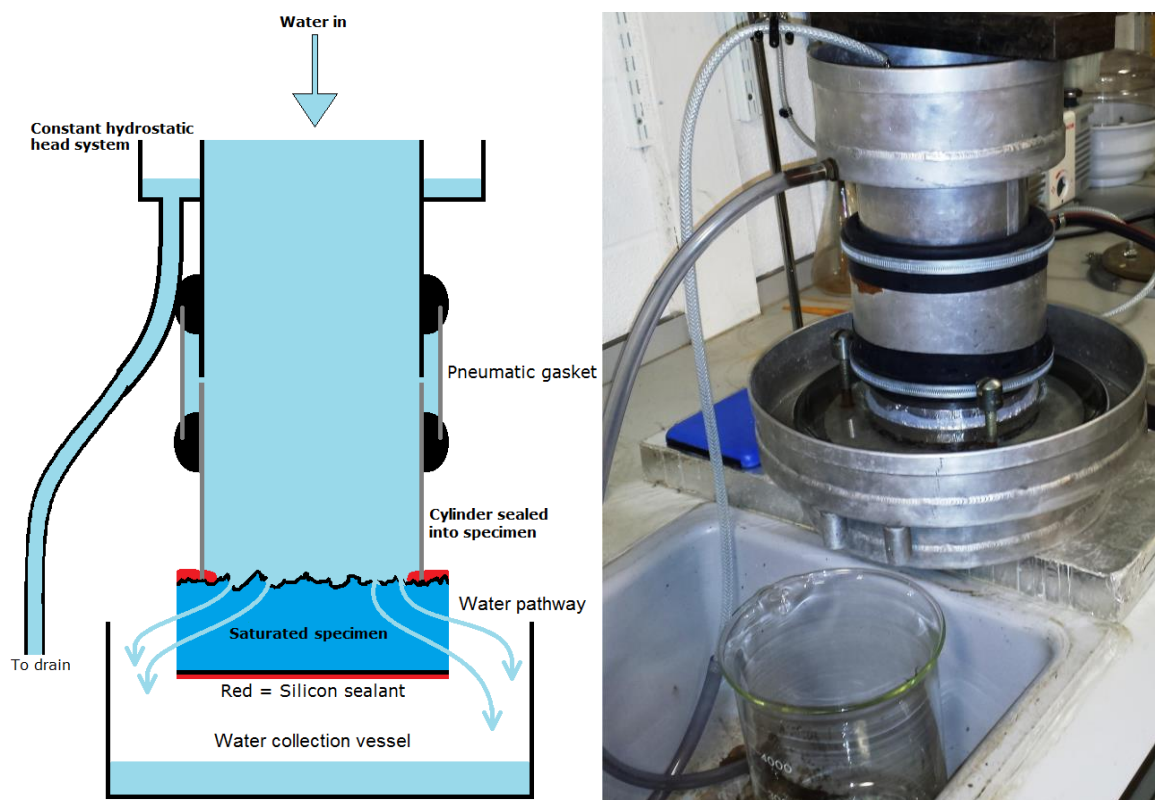
Figure 2-3 Representation of hydraulic permeability setup (left) and the equipment used

3   The relationship between texture depth, permeability and high speed friction

The results from the permeability, high speed friction and texture depth measurements are presented graphically in Figure 3-1, included with these results are the measurements made as part of TRL367 to add context to the data. The colour of the series markers represents the coarse aggregate size and the shape the permeability of the specimen. The cluster of measurements representing the 6 mm TSCS materials has been highlighted by the red circle.
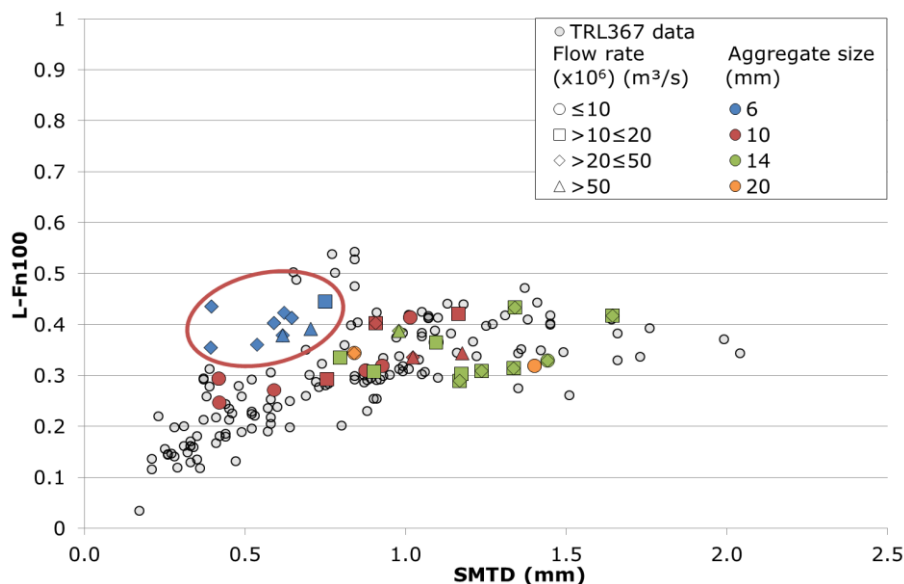
Figure 3-1 Relationship between texture, high speed friction and permeability

If the hypothesis forming the basis of this work is true then it should be expected for the positions of the series markers to move closer to the bulk of the TRL367 measurements when the effects of texture depth and permeability are combined.

This assessment was carried out by augmenting the texture depth, side-force coefficient and friction relationship reported in TRL367 so that the effect of texture depth and permeability are considered additive, this is expressed in Equation 3-1.

$$Predicted\ L - Fn100 = 0.00337SR + 0.411\left(1 - e^{(SMTD+(x \times Flow))}\right) - 0.151$$

Where:

- SR represents the side-force coefficient measured using SCRIM

- SMTD is the texture depth of the (mm)

- x represents the magnitude of the effect of the permeability

- Flow is the flow rate derived from the permeability assessments (mm^3/s).

Equation 3-1 Prediction of L-Fn100 from SR, SMTD and permeability

The magnitude of the effect of the permeability (x) was derived using the conversion of fixed point iteration process which compared the measured friction values with the friction values predicted from Equation 3-1 whilst varying the "x" constant. The best relationship between the measured and predicted values was identified with an x constant value of 10201 units. This has the following effect on Equation 3-1.

$$Predicted\ L-Fn100 = 0.00337SR + 0.411\bigl(1 - e^{(SMTD+(10201\times Flow))}\bigr) - 0.151$$

Equation 3-2 Prediction of L-Fn100 from side-force coefficient, texture depth and permeability with the derived magnitude of flow rate

To demonstrate the effect of permeability, Figure 3-2 shows the friction and texture relationship but the primary x-axis units have been changed to include the flow rate term used in Equation 3-2, the TRL367 data are presented on the secondary x-axis which reports texture depth only. The red circle highlights the position of the 6 mm TSCS when texture depth only is considered so that the change in characterisation can be easily observed.
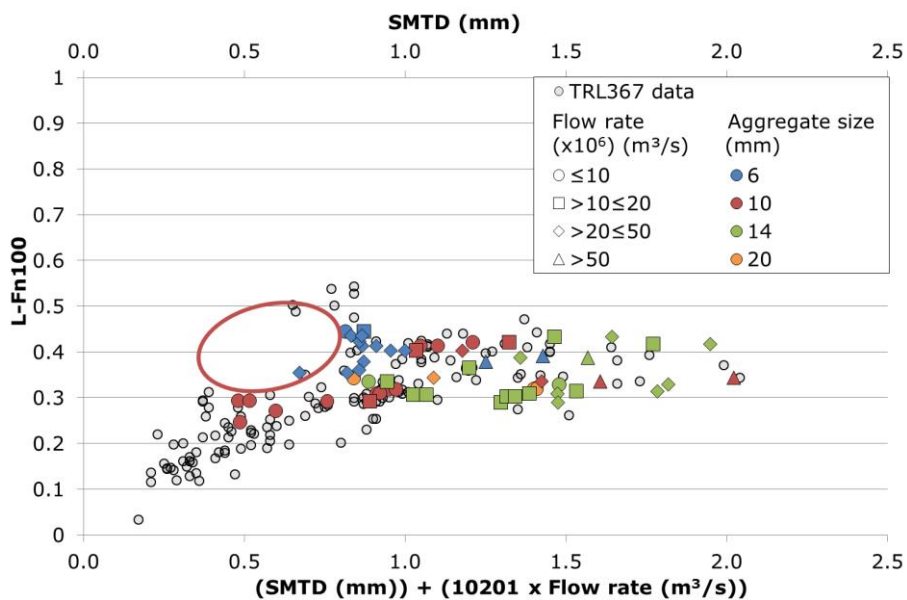
Figure 3-2 Relationship between texture, high speed friction and corrected permeability

The most notable aspect of Figure 3-1 and Figure 3-2 is that the group of 6 mm surfacings (the blue series) have moved out of the red circle and closer to the bulk of the measurements. The positions of other high flow rate materials (the diamond and triangle series) have also moved to the right of the x-axis. Lower flow rate materials however (the round and square series) have moved relatively little.

These observations are in agreement with the original hypothesis and demonstrate a good correlation between the combined effects of texture depth and permeability.

4 Further investigations into permeability

The data presented in Chapter 3 demonstrate a correlation between texture depth, permeability and friction. Furthermore, being a wet test, the horizontal permeability methodology directly links the permeability of the specimens with their ability to remove water from the pavement surface. In order to gain a fuller understanding of permeability, further investigations were carried out into the internal structure of the materials assessed. This chapter presents the findings of a study utilising Computational Topography (CT) to investigate the internal void network of the materials.

This investigation aimed to quantify the relationship between the inter-connectivity of the void network and the total number of voids in the materials assessed. Furthermore this investigation sought to understand the relationship between the interconnectivity of the void network and the flow rates observed from the laboratory testing.

4.1 Materials assessed

Project constraints limited the number of CT assessments that could be carried out, so to gain the most value from the assessments the following specimens were selected:

- Site 6, Section 2, 10mm, Lane 2, Specimen 1 – Highest permeability
- Site 4, Section 3, 20mm, Lane 1, Specimen 2 – Lowest permeability
- Site 5, Section 1, 6mm , Lane 1, Specimen 2 – Permeability closest to the mean
- Site 4, Section 4, 6mm, Lane 1, Specimen 2 – Low texture depth and high friction
- Site 4, Section 2, 10mm, Lane 1, Specimen 1 - Low texture depth and low friction

Figure 4-1 shows the performance of the materials selected. The diamond series markers represent the texture depth performance of the specimen only. The circular markers represent the performance of the specimens when texture depth and permeability are combined, large changes in performance are indicated by the black arrows.
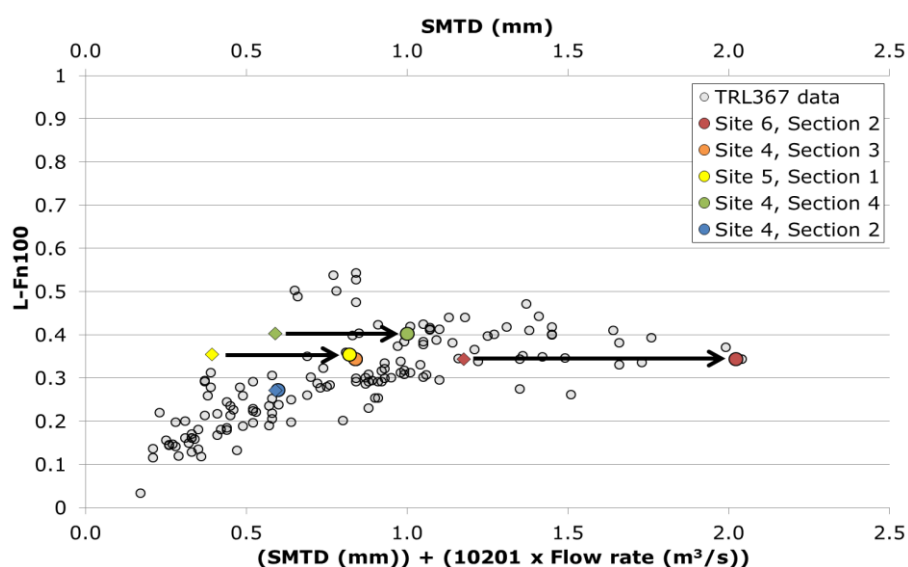
Figure 4-1 Texture depth, permeability and high speed friction of selected specimens

4.2   Measurements made

Computational topography utilises multiple x-ray images which, when combined, provide a three dimensional representation of the internal structure of an object. The collection of x-ray images can be thought of in a similar way to that of photography as both systems utilize the properties of the electro-magnetic spectrum of radiation. In photography a light source emits visible light (wavelength 400 nm to 700 nm) which is partially absorbed and partially reflected by the target object, the reflected light is then captured by a detector in a camera creating a photograph.

The same is true for x-ray imaging, a radioactive source emits x-rays (wavelength 0.01 nm to 10 nm), however because of their shorter wavelength than visible light, some x-rays are absorbed and some pass through the target. The x-rays that pass through a target are captured by a detector creating an image that reveals the internal structure of the target; such an image is known as a radiograph (Figure 4-2). When a number of radiographs are collected at different angles to the target, they can be combined using image processing software to create a three dimensional description of the target.

4.2.1   Specimen preparation and equipment setup

The assessment of road surfacings by CT is relatively rare and so some initial investigations were required to identify the best setup for image collection. Initial imaging was carried out on the specimens used for the permeability testing (150 mm diameter cores). However, it became evident that the density of the specimens was so great that the x-rays could not provide the contrast required for CT. To obtain the required contrast three procedures were carried out:

1. The specimens were mounted at a 30 degree angle to the radiation source to reduce the thickness of material at certain angles of rotation.

2. An 8mm tin filter was added to the radiation source to allow only the highest energy x-rays to be captured by the detector.

3. The specimens were re-sized to a diameter of 100 mm, reducing the overall volume of material.

The effect of these changes was substantial and allowed the collection of high contrast images for analysis.

4.2.2   Image capture

The imaging of the specimens was conducted at the Nikon metrology laboratory in Hertfordshire, UK, using the XT H 450 system. This system utilises a 450 kV radiation source and is capable of producing images to a repeatability and accuracy of 25 microns. To provide sufficient images for CT analysis, 3064 radiographs were made of each specimen by rotating the specimen about an axis perpendicular to the source; one radiograph was therefore made every 0.12 degrees. An example of this is given in Figure 4-2.

Figure 4-2 Example of a captured radiograph (Site 4, Section 3)

The collection of radiographs were then combined using Volume Graphics VGStudio MAX software to create a three dimensional representation of the specimen, this is known as a reconstruction. Figure 4-3 gives an example of the reconstruction for the Site 4, Section 3 specimen. The bottom right panel provides a representation of the exterior of the specimen. The top left, top right and bottom left panels represent the top, side and front view of the specimen in relation to the orientation shown in the bottom right panel. Each slice represents the internal structure of the material at a certain plane in the specimen's depth.
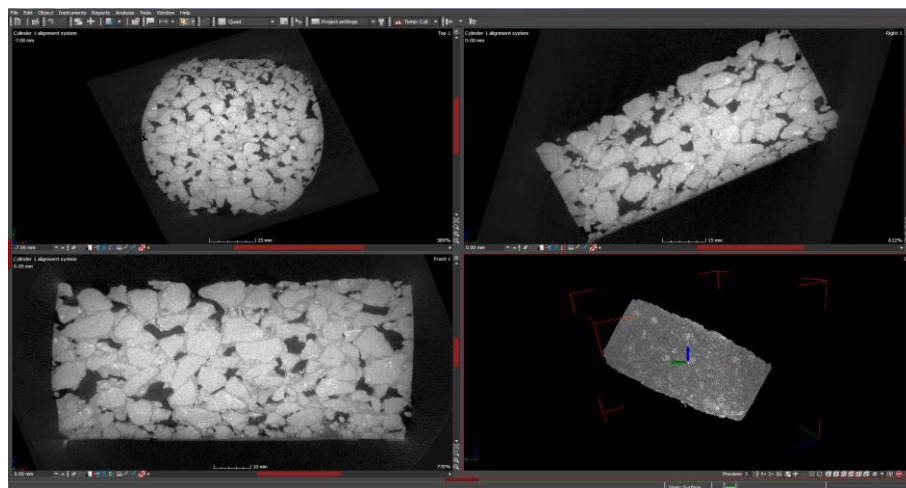
Figure 4-3 Reconstruction of the Site 4, Section 3 specimen

The front slice of the reconstruction is presented in larger scale in Figure 4-4. This level of detail clearly shows the three elements of the material, the aggregate, bitumen binder and air voids, as highlighted by the arrows. The white specks in the image are metallic features within the aggregate particles.

It is interesting to note that the left and right edges of the specimen appear slightly distorted. This is an effect of the imaging process known as "top hatting" and is related to the scatter of x-rays at the edges of dense materials.
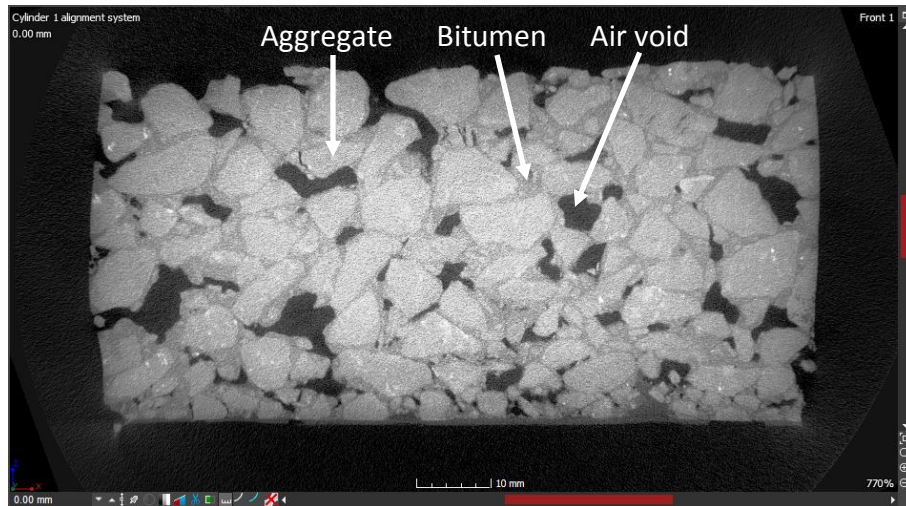
Figure 4-4 Front panel (bottom left) from Figure 4-3

4.3   Image processing

In order to characterise the properties of the specimens, six images were taken from the reconstructions of each specimen. Images were taken from the front perspective of the specimen with the vertical axis set so that it was nominally perpendicular to the surface of the specimen. The depth of the image slice was set so that the middle of the specimen was viewed. This allowed the specimen to be rotated about the vertical axis and images taken at 30 degree increments of rotation. All of the images taken were on the scale of 27 pixels / mm to ensure geometric consistency.

For each of the gathered images the following process was followed in order to determine the area of each image relating to:

- Material, aggregate or bitumen

- A connected air void, an air void that connects to the surface through the network of inter-connected voids

- An isolated air void, an air void that does not connect to the surface, but may be part of a network of inter-connected voids

Cropping and rotation

The first step was to rotate the images so that any variations in the angle of the surface relative to the vertical axis were removed. This was carried out by using the Adobe Photoshop CS2 image processing suite to rotate the image until the surface was horizontal. The image was then cropped so that the following conditions were met:

- The distance between the top of the highest aggregate protrusion and the top of the image was 0.5 mm

- The width of the image represented the middle 90 mm of the specimen

- The height of the image equated to 40 mm

This process ensured that all of the images assessed were representative of the same amount of each specimen. A secondary effect was to reduce the top hating effect by cropping the distorted edges. An example of a captured, and cropped and rotated image is provided in Figure 4-5 and Figure 4-6.
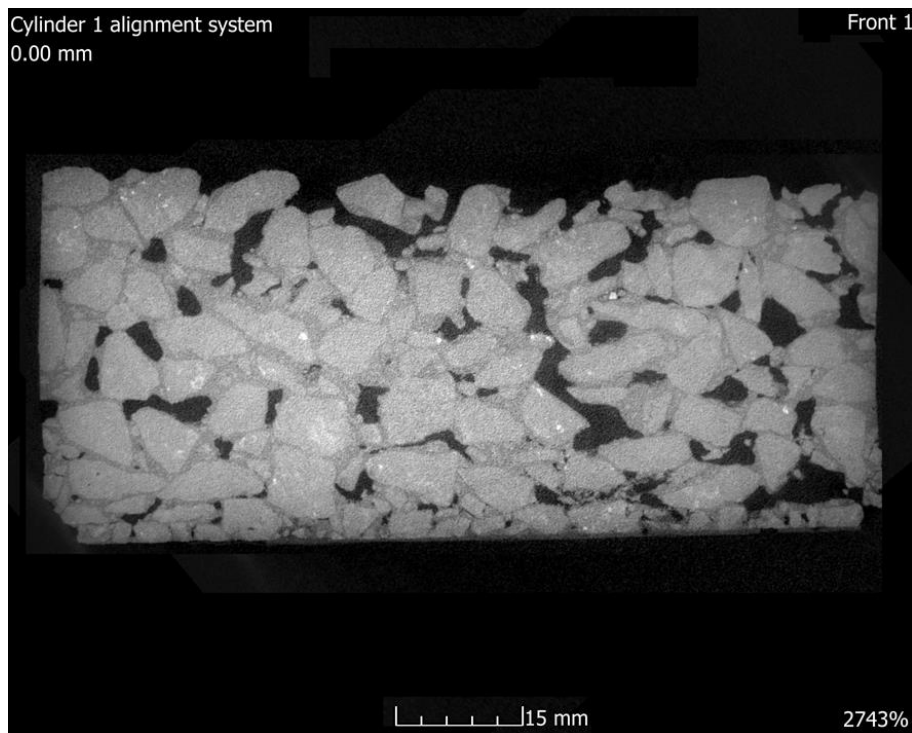
Figure 4-5 Example of a captured image
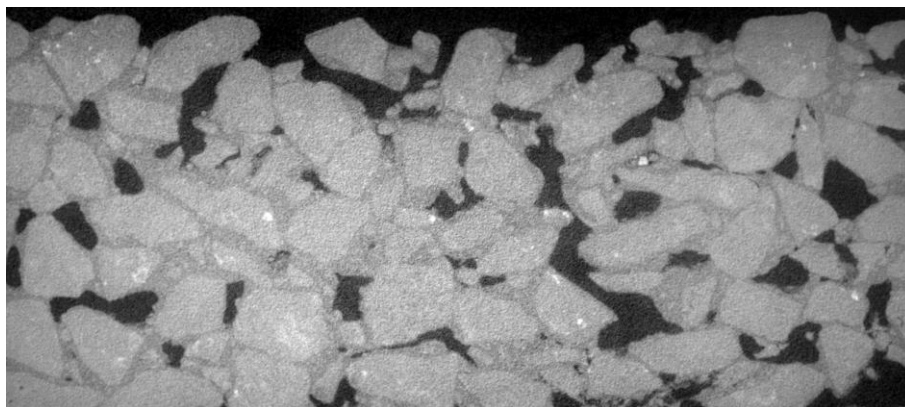
Figure 4-6 Example of a cropped and rotated image

Conversion to a binary image

The cropped and rotated images were then converted to a black and white image such that white areas represented the material and black areas represented air voids. Differences in image contrast between the edges and centre of the image meant that a single threshold could not be applied to identify dark (air voids) and light (material) regions. To overcome this issue a manual operation was used utilising the "Magic wand tool" in the Photoshop CS2 suite. The tool was set to a tolerance of 80% and the middle of an air void region selected. The magic wand tool then selected an area of pixel intensity values within 80% of the selected value. The luminosity of the selected area was then reduced so that the void was represented by an area of zero value intensity pixels.

This procedure was repeated for every air void location in every image. The final step of the procedure was to use the magic wand tool to select every non-zero pixel value (areas representing material). The luminosity of these areas was then increased so that they were represented by areas that were white. This process created a series of images as per the example in Figure 4-7

Figure 4-7 Example of a binary image

Tracing and void characterisation

The final stage of the image processing was to characterise the air voids into connected (a void that connects to the surface) and isolated (a void that does not connect to the surface). This characterisation was carried out manually using a process referred to here as tracing. During the tracing process if a void was identified as connected then it was coloured blue, and if it was identified as isolated it was coloured pink[5]. This created an image as per the example in Figure 4-8.

---

[5] The coloring process was carried out using the "fill" tool in Microsoft paint.

Using the Volume Graphics MyVGL software the tracing process was carried out on the reconstructed CT images using the following process:

- The orientation of the reconstructed specimen and slice depth was set to that of the original image.

- The slice step length was set to 0.10 mm.

- The operator selected a void to assess and incrementally increased the depth of the slice, following the progression of the void through the image until the edge of the specimen was found. If no connection to the surface could be found then the process was repeated but reducing the slice depth.

- If a connection between the selected void and the surface could be found then the void in the binary image was coloured accordingly.

This process was repeated for every void in every image. The resulting collection of traced images therefore contained three pieces of information, the vertical and horizontal geometry of the voids, and a binary representation of their connected states.

Figure 4-8 Example of a traced image

Conversion to numerical values

Following the image processing stages, the traced images were converted into a matrix of pixel intensity values using a bespoke software package. The matrices were created such that the position of the value in the matrix represented its location in the image and the magnitude of the value related to its colour:

- Blue (connected voids) = 339

- White (material) = 765

- Pink (isolated voids) = 630

4.4   Assessment of data

The matrices of pixel intensity values produced by the analysis of the CT images were used to characterise the following material properties for each specimen:

- the amount of material

- the amount of connected voids

- the amount of isolated voids

- the amount of total voids

Each material property was characterised by the average percentage of each image that represented the above properties.   The remainder of this section describes the characterisation process.

4.4.1   *Quantification of surface effects*

In order to ensure that only the internal structure of the material was included in the characterisations, it was necessary to quantify and remove any surface effects. For the purpose of this exercise a surface effect was considered as any void that could be viewed from a vertical viewpoint above the specimen. This is illustrated in Figure 4-9 which shows a traced image but the surface effects are presented in green.

Figure 4-9 Demonstration of the removal of surface effects

Quantifying these effects was achieved by counting the number of consecutive rows in a column that contained connected voids (a number of 339 in the matrix) starting from the top row. The sum of the row counts for each column provided the quantification of surface effects.

4.4.2 Quantifying the amount of material and void types

For each matrix the number of cells representing material, isolated voids and connected voids, and total voids were calculated by counting the number of cells in the image matrix equating to each of these states:

- Material (M) = number of cells with value "765"

- Isolated Voids (IV) = number of cells with value "630"

- Connected Voids (CV) = number of cells with value "339" minus the contribution of surface effects

- Total voids (TV) = number of cells with value of "339" or "630" minus the contribution of surface effects

Based on these values the Area Of Interest (AOI) (the amount of the image matrix not relating to surface effects) was calculated using Equation 4-1, this will act as a reference against which the percentage of the AOI represented by each of the above variables could be defined.

$$Area\ Of\ Interest\ (AOI) = M + IV + CV$$

$$\%\ of\ AOI\ containing\ variable = \frac{100 \times Variable}{AOI}$$

Equation 4-1 Calculation of AOI for a single matrix and the percentage of each variable that contributes to it

To gain an overall characterisation for each specimen, a mean of the percentage of the AOI represented by each variable was taken for all of the matrices representing a single specimen. These averages are the final characterisations that were used in the analysis stage:

- Average % material

- Average % isolated

- Average % connected

- Average % voids

A full account of the results of the analysis of CT images can be found in Appendix C. The following chapter presents the salient findings.

5 The relationship between internally connected voids, flow rate and total void content

The results of the CT imaging and laboratory testing were used to assess the relationship between the horizontal permeability of the specimens and the prevalence of interconnected voids. In addition the relationship between the prevalence of interconnected voids and all voids was assessed in order to further understand the behaviour of porous materials.

5.1 Connected voids and horizontal permeability

The relationship between the horizontal permeability of the specimens and their prevalence for possessing connected voids is shown in Figure 5-1. The black series markers represent the percentage of connected voids calculated from each of the six images taken from a specimen. The blue markers represent the mean of these measurements and the blue line is the line of best fit through the mean values.

There are two key features observed from Figure 5-1, the first is a large amount of scatter in the measurements made on individual images. This is particularly prevalent for the images assessed from the specimen taken from Site 5, Section 1 (permeability closest to the mean) where the percentage of connected voids was calculated between 2.4% and 9.4%. The observed scatter may be a product of the manual analysis of the images that was carried out through the tracing process. A computational approach may yield more repeatable results[6].

The second feature is that despite the scatter in the individual measurements a good correlation is observed between the average percentage of connected voids, and the horizontal permeability. This observation is key as it confirms that the mechanism of horizontal permeability is through the inter-connected void network of the specimens.
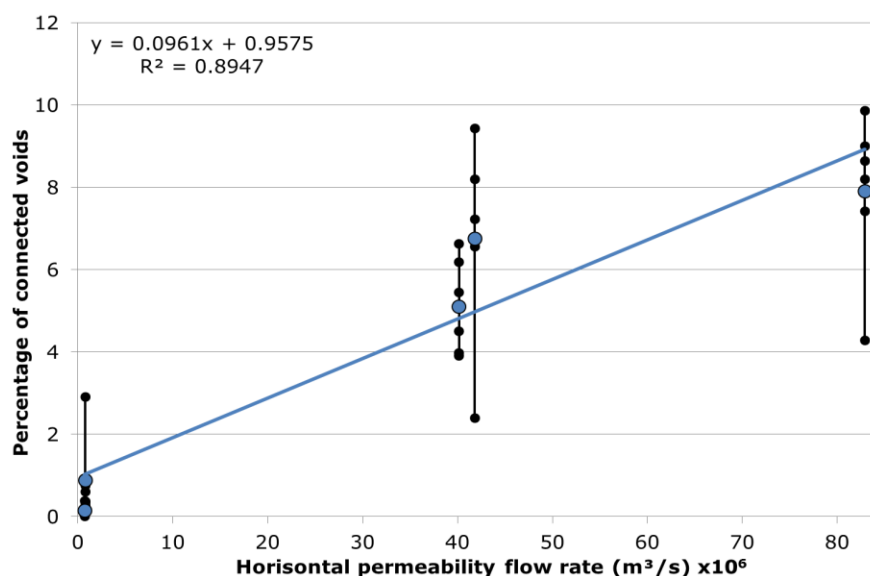
Figure 5-1 The relationship between horizontal permeability and connected voids

---

[6] A computational approach would take computing power several orders of magnitude greater than that which was immediately available and procuring such devices would have exceeded the financial limits of the project.

5.2   Connected voids and total voids

Figure 5-2 presents the relationship between the percentage of all voids in a specimen (connected and isolated) and the percentage of connected voids. The small diamond series represent measurements made on individual images taken from a specimen, and the large circles represent the average of the measurements for a specimen.   The black line represents the line of best fit with the average values. The colour of the series is used to identify measurements made on different specimens.

The key observation from Figure 5-2 is an excellent relationship between the average of all voids and connected voids for the materials assessed.   This observation suggests that because of the randomly orientated particles in road materials, pavements with high void contents have a greater chance of providing an inter-connected void network. Although this observation is made on a relatively small number of measurements, this could be a potentially valuable insight into the behaviour of porous materials.
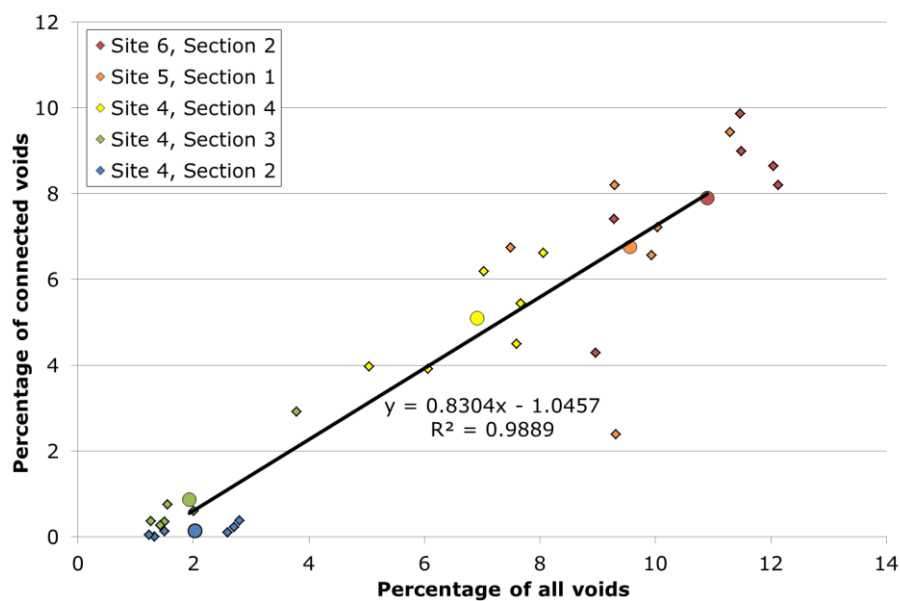
Figure 5-2 The relationship between all voids and connected voids

6 Discussion and conclusions

6.1 Permeability, texture depth and high speed friction

The key hypothesis for this work was that a pavement may remove water from the tyre road interface either via the surface texture depth or through the internal permeability of the surfacing; both mechanisms aid the pavement in providing high speed locked-wheel friction. Through the research tasks listed in chapter 1 this hypothesis has been shown to be valid.

The relationships observed between texture depth, horizontal permeability and high speed friction have demonstrated that the removal of water from the tyre surface interface is a key property in the generation of high speed friction. This has confirmed the previous thinking established in TRL367 (Roe, et al., 1998). For the specimens assessed the CT imaging has shown that the mechanism for the removal of water from the tyre surface interface is through an interconnected network of voids through the pavement structure.

The analysis of the CT images has also demonstrated the possibility that an inter-connected void network is an inevitable result of constructing pavements with a high void content. That is to say that pavements with a high void content will provide some voids which are isolated and some that are connected and that the greater the overall void content the greater the number of connected and isolated voids.

6.2 The characterisation of high speed friction performance

The current methodology used in the UK for mitigating the risks posed to motorists resulting from poor high speed friction relies on the relationship between texture and high speed friction developed in TRL367, which has shown to be inappropriate for some materials. However for the bulk of materials this relationship works well and fails-safe for those materials where the relationship is invalid.

The current methodology means that for certain materials the validation of high speed friction performance must be carried out directly by making measurements using specialist equipment. The methodology used in this work for characterising horizontal permeability may offer an alternative means of characterising the performance of these materials.

An alternative approach would be to allow the option of making measurements of texture depth and permeability in the place of high speed friction. For instance, materials with a texture depth of 0.40 mm SMTD could be accepted if their horizontal flow rate is within a certain range measured according to the technique described in BS EN 12697-19:2012[7].

A re-writing of the standards in this way would require careful consideration as although the relationships described here are robust and should provide a sufficient estimate of high speed friction, there are other properties related to permeability that could produce an adverse effect. One property requiring consideration is the durability of the structure of the pavement. Previous works have shown that porous pavements can be expected to provide lower service lives than non-porous pavements. This is due to the ingress of water into the

---

[7]The technique used to characterize horizontal flow rate for this work

pavement affecting the bonds between pavement particles through the freeze thaw effect or hydraulic pressure.

Another effect worth consideration is the longevity of the porosity of the pavement itself. It is possible that over time, detritus could cause the voids in a porous pavement to become clogged. In this case the ability of the pavement to remove water from the surface may be compromised, negating the benefits for high speed friction. This phenomenon may warrant further research to investigate the potential for this effect in different environments and the timescales evolved.

6.3   Conclusions

From the work carried out the following conclusions can be made:

- A key characteristic influencing high speed locked-wheel friction in wet conditions is the ability of the pavement to remove water from the tyre / road interface.

- The major pathway for water removal from the tyre / road interface is through the surface texture, but the inter-connected void network can provide additional drainage routes.

- There is an indication that pavements with a large percentage of voids inevitably possess a large number of inter-connected voids.

- There is the possibility of amending current standards which require measurements of high speed friction, to allow an inference of high speed friction based on the measurement of texture and permeability.

Bibliography

ASTM, 2008. *E524-08 Standard Specification for Standard Smooth Tire for Pavement Skid-resistance Tests,* West Conshohocken: ASTM.

ASTM, 2011. *E274/E274M-11 Standard Test Method for SkidResistance of Paved surfaces Using a full-Scale Tire,* West Conshohocken: ASTM.

British Standards, 2004. *BS EN ISO 13473-1:2004 Characterisation of pavement by use of surface profiles - Part 1 - Determination of MPD,* London: BSI.

British Standards, 2010. *BS EN 13036-1. Road and airfield surface characteristics - Test methods. Part 1: Measurement of pavement surface macrotexture depth using a volumetric patch technique,* London: BSi.

British Standards, 2012. *BS EN 12697-19:2012 Bituminous mixtures - test methods for hot mix asphalt part 19: Permeability of specimen,* London: BSI.

Highways England, Transport Scotland, Welsh Government, The Department for Regional Development Northern Ireland, 2008. *HD29/08 - Data for pavement assessment,* London: The Stationery Office.

Highways England, Transport Scotland, Welsh Government, The Department for Regional Development Northern Ireland, 2008. *Manual of Contract Documents for Highway Works (MCHW), Volume 2, Series NG 0900,* London: The Stationery Office.

Highways England, Transport Scotland, Welsh Government, The Department for Regional Development Northern Ireland, 2012. *Interim advice note 154/12,* London: The Stationery Office.

Leu, M. C. & Henry, J. J., 1978. *Prediction of skid resistance as a function of speed from pavement texture measurements,* Washington: Transportation Research Board.

Ordnance Survey, n.d. *Ordnance survey open data.* [Online]
Available at: http://www.ordnancesurvey.co.uk/oswebsite/opendata/
[Accessed 02 09 2011].

Roe, P. G. & Dunford, A., 2012. *PPR564 The skid resistance behaviour of thin surface course systems,* Wokingham: HA / MPA / RBA Collabarative Programme 2008-11: topic 1 prepared for Highways Agency, Minerals Products Association and Refined Bitumen Association.

Roe, P. G., Dunford, A. & Crabb, G., 2008. *PPR324 HA/QPA/RBA Collaborative Programme 2004/07: Surface requirements for asphalt roads,* Wokingham: TRL.

Roe, P. G., Parry, A. R. & Viner, H. E., 1998. *TRL367 High and low speed skidding resistance: the influence of texture depth,* Wokingham: Prepared for Pavement Engineering Group, Highways Agency.

Sabey, B. E., 1966. *RRL20 Road surface texture and the change in skidding resistance with speed,* Wokingham: Road Research Laboratory.

Sanders, P. D., Morosiuk, K. & Peeling, J. R., 2014. *PPR727 Road surface properties and high speed friction,* Wokingham: TRL.

Viner, H. et al., 2006. *PPR148, Surface texture measurements on local roads.,* Crowthorne: TRL Ltd.

Appendix A   Site locations

This appendix presents the locations of the sites tested. Each map contains the lengths of each numbered section and the end of the last section, donated by the "E" marker.
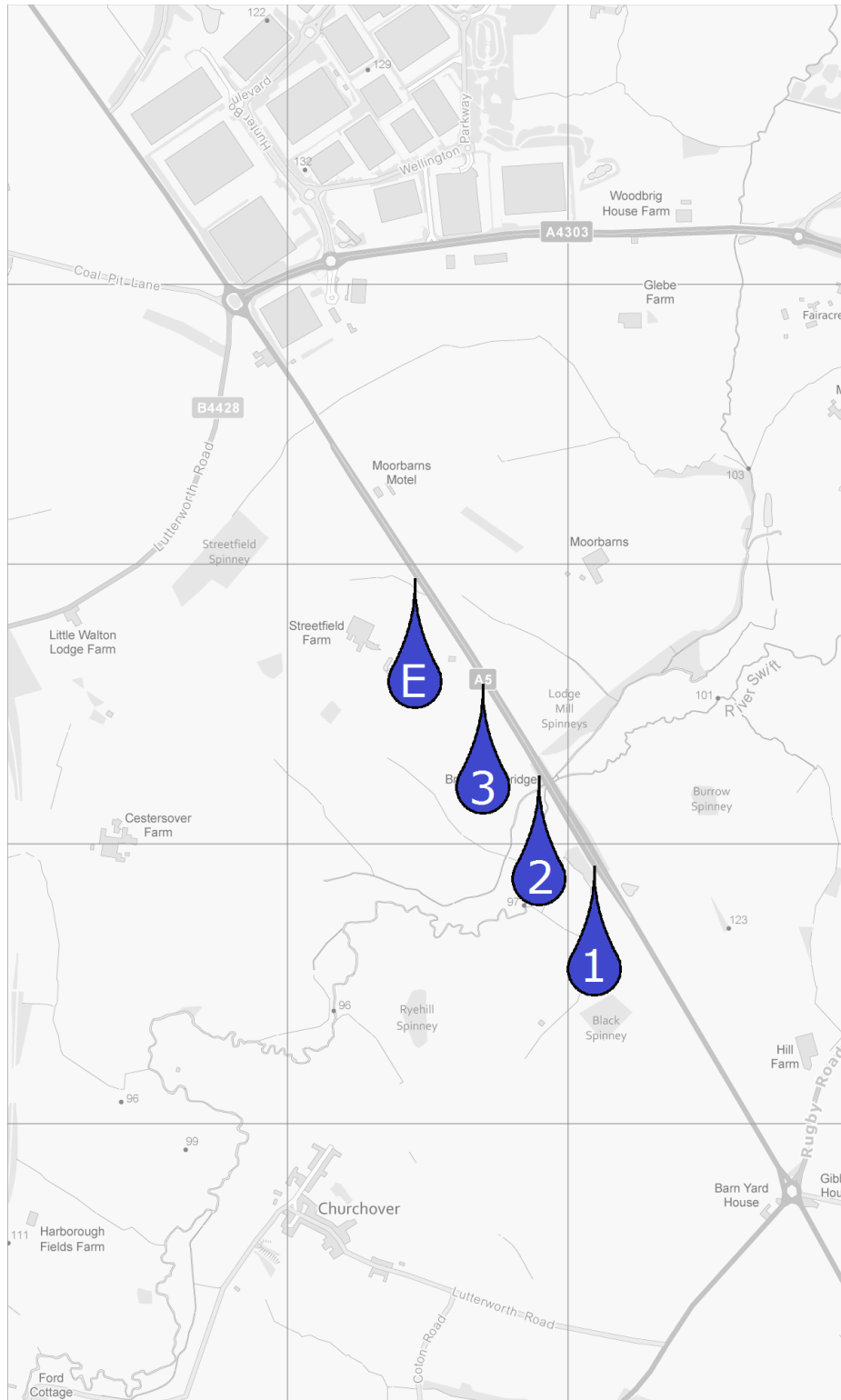
Figure B - 1 Site 1

Figure B - 2 Site 2
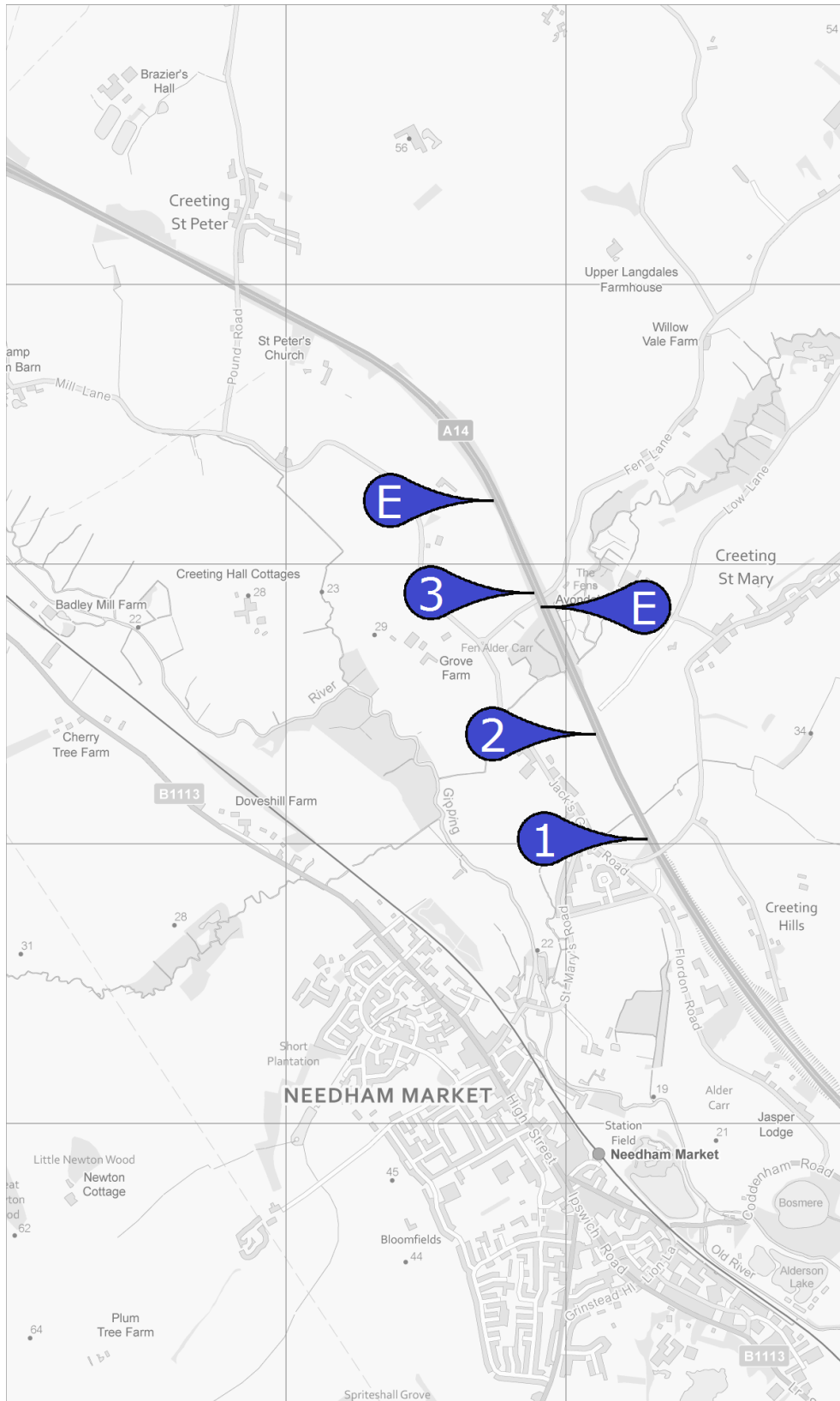
Figure B - 3 Site 3
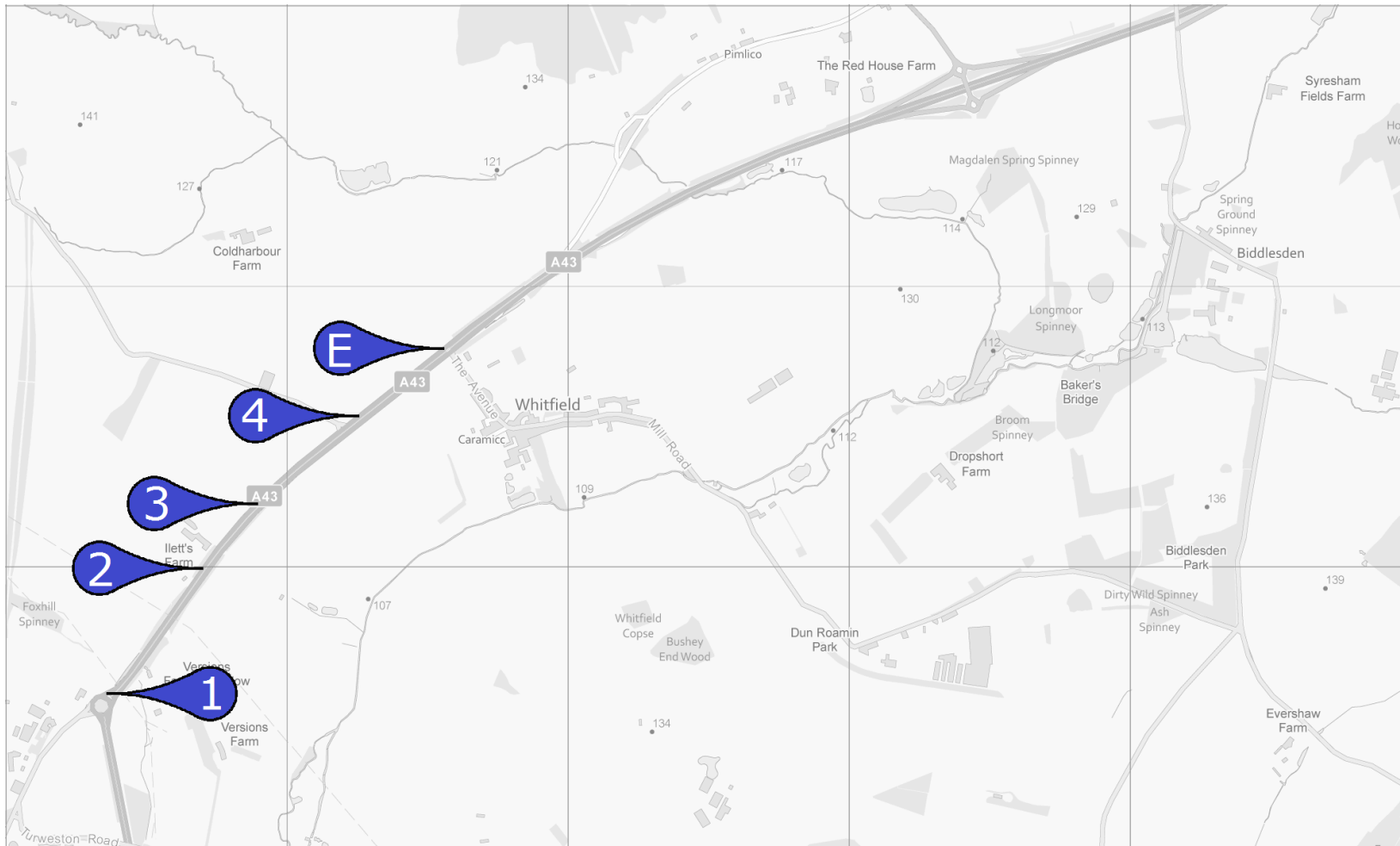
Figure B - 4 Site 4

Figure B - 5 Site 5
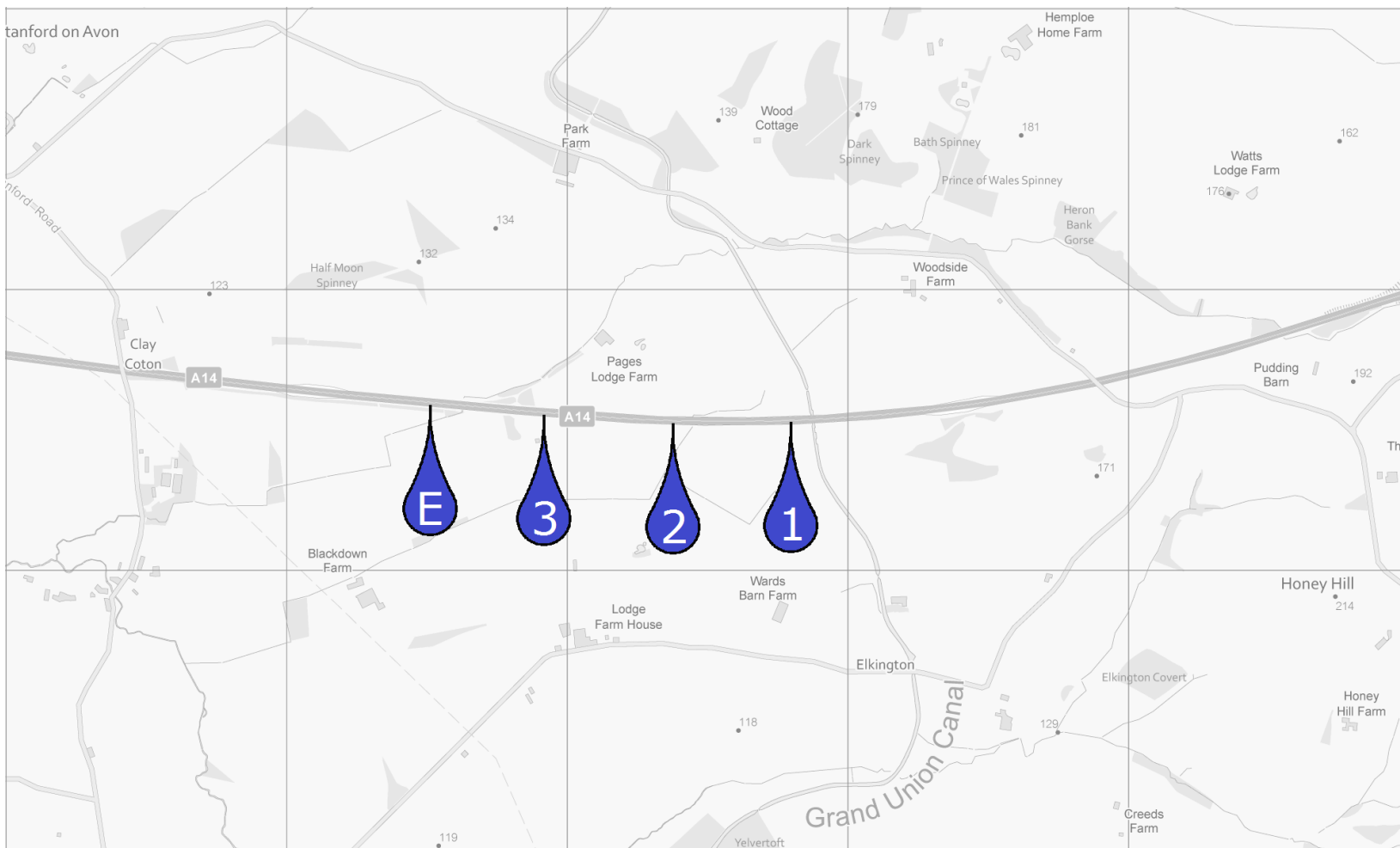
Figure B - 6 Site 6

Appendix B   Results of full scale and laboratory measurements

Table B - 1 presents the results of the measurements made as part of the laboratory and full scale assessments. The flow rate for each specimen is provided as are the texture depth, side-force coefficient, and high speed friction values derived for each parent surface.

Table B - 1 Results from full scale and laboratory assessments

	Material description							
Site	Section	Coarse aggregate size (mm)	Lane	Specimen No.	SMTD (mm)	L-Fn100	SR(50)	Flow rate (m³/s)
1	1	10	1	1	0.91	0.40	69.23	1.26E-05
				2	0.91	0.40	69.23	2.66E-05
			2	1	1.16	0.42	73.68	1.57E-05
				2	1.16	0.42	73.68	4.56E-06
	2	6	1	2	0.62	0.42	72.24	2.31E-05
			2	1	0.75	0.44	73.93	1.19E-05
				2	0.75	0.44	73.93	6.29E-06
	3	14	1	1	1.09	0.37	65.17	9.91E-06
				2	1.09	0.37	65.17	1.02E-05
			2	1	1.34	0.43	73.93	1.22E-05
				2	1.34	0.43	73.93	2.98E-05
2	1	14	1	1	1.17	0.30	57.05	1.65E-05
				2	1.17	0.30	57.05	1.39E-05
			2	1	1.64	0.42	62.65	2.98E-05
				2	1.64	0.42	62.65	1.25E-05
	2	10	1	1	0.75	0.29	60.21	3.15E-07
				2	1.01	0.41	66.87	3.35E-06
			2	1	1.01	0.41	66.87	8.50E-06
				2	0.75	0.29	60.21	1.33E-05
3	1	14	1	1	1.17	0.29	55.82	1.28E-05
				2	1.17	0.29	55.82	3.01E-05
	2	10	1	1	0.88	0.31	59.50	3.61E-06
				2	0.88	0.31	59.50	4.52E-06
	3	6	1	1	0.62	0.38	65.90	6.21E-05
				2	0.62	0.38	65.90	2.49E-05
4	1	14	1	1	0.90	0.31	57.24	1.61E-05

				2	0.90	0.31	57.24	1.22E-05
			2	1	1.34	0.31	63.07	1.93E-05
				2	1.34	0.31	63.07	4.40E-05
	2	10	1	1	0.59	0.27	62.27	7.32E-07
			2	1	0.93	0.32	64.93	2.05E-06
				2	0.93	0.32	64.93	4.29E-06
	3	20	1	1	0.84	0.34	59.52	2.44E-05
				2	0.84	0.34	59.52	7.97E-08
			2	1	1.40	0.32	65.31	8.24E-07
				2	1.40	0.32	65.31	6.55E-09
	4	6	1	1	0.59	0.40	68.05	3.58E-05
				2	0.59	0.40	68.05	4.02E-05
			2	1	0.65	0.41	68.33	2.17E-05
				2	0.65	0.41	68.33	2.60E-05
5	1	6	1	1	0.39	0.35	57.90	2.73E-05
				2	0.39	0.35	57.90	4.18E-05
	2	10	1	1	0.42	0.29	62.26	6.22E-06
				2	0.42	0.29	62.26	9.66E-06
	3	14	1	1	0.80	0.33	57.65	1.45E-05
				2	0.80	0.33	57.65	8.83E-06
	4	6	1	1	0.40	0.44	68.79	4.28E-05
				2	0.40	0.44	68.79	4.61E-05
	5	10	1	1	0.42	0.25	72.20	6.45E-06
	6	14	1	1	0.98	0.39	65.67	3.72E-05
				2	0.98	0.39	65.67	5.78E-05
6	1	6	1	1	0.54	0.36	67.34	3.13E-05
			2	2	0.70	0.39	59.01	7.10E-05
	2	10	1	1	1.02	0.34	60.12	3.94E-05
				2	1.02	0.34	60.12	5.73E-05
			2	1	1.18	0.34	58.84	8.29E-05
	3	14	1	1	1.24	0.31	57.82	2.33E-05
				2	1.24	0.31	57.82	1.47E-05
			2	1	1.44	0.33	60.75	3.69E-05
				2	1.44	0.33	60.75	3.66E-06

Appendix C   Results of CT imaging

Table C- 1 Full results from analysis of CT imaging

Specimen	Image angle of rotation (degrees)	% Material	% Isolated voids	% Connected voids	% Total voids	Average % material	Average % isolated voids	Average % connected voids	Average % total voids
	0	90.07	3.37	6.56	9.93				
	30	92.50	0.76	6.74	7.50				
	60	89.96	2.83	7.22	10.04				
Site 5, Section 1	90	88.71	1.86	9.43	11.29	90.44	2.81	6.76	9.56
	120	90.68	6.93	2.39	9.32				
	150	90.70	1.10	8.20	9.30				
	0	87.87	3.93	8.20	12.13				
	30	90.71	1.87	7.41	9.29				
	60	87.96	3.40	8.64	12.04				
Site 6, Section 2	90	88.52	2.49	8.99	11.48	89.10	3.00	7.90	10.90
	120	91.04	4.68	4.29	8.96				
	150	88.53	1.61	9.86	11.47				
	0	98.67	1.32	0.00	1.33				
	30	97.41	2.48	0.11	2.59				
	60	97.30	2.48	0.23	2.70				
Site 4, Section 2	90	97.20	2.42	0.38	2.80	97.97	1.88	0.15	2.03
	120	98.50	1.38	0.12	1.50				
	150	98.77	1.19	0.05	1.23				
Site 4, Section 4	0	92.96	0.86	6.18	7.04	93.09	1.81	5.10	6.91

	30	92.33	2.23	5.45	7.67			
	60	92.40	3.11	4.50	7.60			
	90	91.94	1.44	6.62	8.06			
	120	93.94	2.15	3.91	6.06			
	150	94.95	1.07	3.98	5.05			
Site 4, Section 3	0	98.50	1.15	0.35	1.50	98.07	1.05	0.87	1.93
	30	97.99	1.41	0.60	2.01			
	60	98.57	1.16	0.27	1.43			
	90	96.21	0.88	2.91	3.79			
	120	98.44	0.80	0.76	1.56			
	150	98.74	0.90	0.36	1.26			

40

Road surface properties and high speed friction - The effect of permeability

Understanding the relationships between road surface properties and high speed friction is key to managing the risk of loss of vehicle control. It is understood that, in wet conditions, texture depth plays an important part in the generation of locked-wheel high speed friction. For the majority of road surfacing materials low levels of texture depth are likely to correlate with low levels of friction. However, this is not the case for all surfaces as previous works have shown there are some surfaces that provide low levels of texture depth and high levels of friction.

The work documented in this report explores the relationship between high speed friction and road surface properties with a view to identifying the mechanisms by which materials can provide low levels of texture depth yet high levels of locked-wheel high speed friction.

Other titles from this subject area

PPR727   Road surface properties and high speed friction. Sanders P D, Morosiuk K, Peeling J R. 2014

PPR564   The skid resistance behaviour of thin surface course systems. Roe P G, Dunford A. 2012

TRL367   High and low speed skidding resistance: the influence of texture depth. Roe P G, Parry A R, Viner H E. 1998

RRL20   Road surface texture and the change in skidding resistance with speed. Sabey B E. 1966